Polymer Chemistry

Accepted Manuscript

ROYAL SOCIETY OF CHEMISTRY

www.rsc.org/polymers

Journal Name

ARTICLE

Nitrile - Substituted Thienyl and Phenyl Units as Building Blocks for High Performance n-Type Polymer Semiconductors

Received 00th January 20xx,
Accepted 00th January 20xx

DOI: 10.1039/x0xx00000x

www.rsc.org/

Yu Xiong, Xiaolan Qiao and Hongxiang Li *

Two novel polymers **PDPP3T-CN** and **PDPPTPT-CN** containing nitrile-substituted thienyl and phenyl units were designed and synthesized. The influence of nitrile groups on the electronic properties and charge-carrier transport of the polymers was thoroughly investigated and highlighted by comparing with the corresponding non-nitrile substituted polymers. Experimental results showed the introduction of nitrile groups lowered the HOMO and LUMO energy levels of polymers about 0.3 eV and 0.2 eV, respectively. Thin film transistors characteristics displayed both polymers exhibited electron-dominated ambipolar behavior in ambient condition. The highest electron/hole mobilities were 0.18/0.0083 $cm^2V^{-1}s^{-1}$ for **PDPPTPT-CN** and 0.09/0.0017 $cm^2V^{-1}s^{-1}$ for **PDPP3T-CN**, one of the highest electron mobility for DPP-based polymers measured in ambient condition with bottom-gate/top-contact device configuration.

Introduction

Due to the excellent solution processability and mechanical flexibility, π-conjugated polymer semiconductors have attracted increasing attentions for their applications in organic field-effect transistors (OFETs).[1-4] Exploration of high mobility polymer semiconductors has continuously been a central object for OFETs research.[5] In recent years, polymer semiconductors with high mobility have been achieved by constructing low band gap copolymers with alternating electron-rich units (donor) and electron-deficient units (acceptor) on the conjugated backbones.[6-14] Till now, the high mobility low band gap polymers reported are mainly p-type semiconductors,[5] for example, impressively hole-mobility of 14.4 $cm^2V^{-1}s^{-1}$ has been realized for thienoisoindigo (TIIG) - naphthalene copolymer.[15] Comparing with the massive high performance p-type polymer semiconductors, much fewer n-type polymer semiconductors have been reported,[16-18] especially the one with high electron mobility and ambient stability. Since the low power complementary circuits are composed of both p-type and n-type OFETs, the development of high performance and ambient stable n-type polymer semiconductors is vital and requirable.[19]

The deficiency of n-type polymer semiconductors is mainly due to the unavailability of suitable electron-deficient building blocks to construct polymers with high electron affinity or a deep lowest unoccupied molecular orbital (LUMO) energy level for facile injection and efficient transport of electrons.[20] Commonly, the strong electron-withdrawing units used in polymer semiconductors are aromatic diimides, benzo[c][1,2,5]thiadiazole and aromatic rings with halogens (especially for fluorine) substituent.[5, 20-23] To develop and find new type of electron-deficient building blocks is crucial for n-type polymer semiconductors. Similar as fluoride and diimde, nitrile is a strong electron withdrawing group. Though nitrile containing conjugation polymers have been used as electron transport materials in OLED, they are rarely to be used in n-type polymer transistors. [24-25] Recently, nitrile group has been introduced onto the vinylene moiety and copolymerized with DPP unit.[18] Though isomer impurities existed, these polymers displayed high electron-mobility, suggesting the potential applications of nitrile group in n-type semiconductors. Inspired by these results, herein, copolymers **PDPP3T-CN** and **PDPPTPT-CN** containing nitrile-substituted thiophene and benzene were designed and synthesized (chemical structures see Scheme 1). The incorporation of nitrile-substituted thiophene and benzene blocks not only effectively lowered the LUMO energy levels of polymers, but also avoided the impurities of isomers. Furthermore, the introduction of nitrile group might be beneficial to enhance intermolecular interactions by forming adjacent intermolecular hydrogen bonds. Experimental results showed the solution processed thin film transistors of **PDPP3T-CN** and **PDPPTPT-CN** exhibited electron-dominated ambipolar behaviour with high electron mobilities up to 0.09 cm^2/Vs and 0.18 cm^2/Vs in ambient with bottom-gate/top-contact device configuration, respectively, demonstrating the applications of aromatic nitrile units in high performance n-type polymer semiconductors.

[a] *Key Laboratory of synthetic and self-assembly chemistry for organic functional molecules, Shanghai Institute of Organic Chemistry, CAS, Shanghai, 200032, China. Email: lhx@mail.sioc.ac.cn*

Electronic Supplementary Information (ESI) available: [TGA and DSC curves, AFM images]. See DOI: 10.1039/x0xx00000x

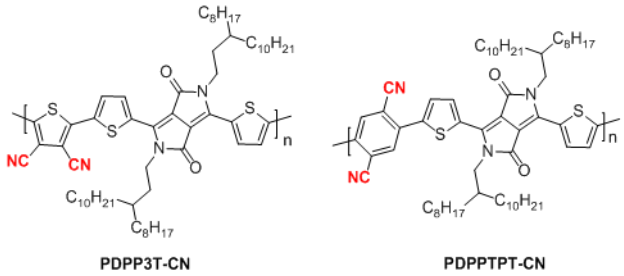

Scheme 1. Chemical structures of polymers **PDPP3T-CN** and **PDPPTPT-CN**

Experimental

General

All reactions were performed under nitrogen atmosphere unless stated otherwise. The monomers and target polymers were identified by ^{1}H NMR (300 MHz, $CDCl_3$: Varian Mercury spectrometer; 400 MHz, $CDCl_2CDCl_2$: Bruker DRX-400 spectrometer), elemental analyses (Vario EL III elemental analyzer) and high temperature gel-permeation chromatography (PL-GPC220 instrument, 150 ℃, using 1,2,4-trichlorobenzene as eluent and polystyrene standards as calibrant).

Cyclic voltammetry (CV) studies were carried out in acetonitrile under nitrogen protection by CHI610D electrochemical workstation. We used Pt disk as working electrode, $Ag/AgNO_3$ as reference electrode, Pt wire as counter electrode and 0.1 M $^n Bu_4NPF_6$ as the supporting electrolyte. Measurements were calibrated with ferrocene (Fc) as the internal standard. UV-vis absorption spectra were recorded on U-3900 spectrophotometer. TGA measurements were conducted on a TA Q500 instrument under a dry nitrogen flow at a heating rate of 10 ℃/min. DSC analyses were performed on a TA Q2000 instrument under nitrogen atmosphere at a heating (cooling) scan rate of 10 ℃/min. AFM was recorded on a Nanoscope IIIa atomic force microscopy (AFM) in tapping mode.

Device Fabrication

The devices were fabricated in top-contact/bottom gate configurations using heavily doped Si wafer as the bottom gate electrode and 300 nm of SiO_2 layer as the gate dielectric. The substrates were cleaned and modified with octadecyltrichlorosilane (OTS) according to the reported procedure.[26] The organic active layer was deposited onto the substrates by a spin-coating process (6 mg/mL in chloroform, 3000 rpm, 30s) under atmosphere. The Au source and drain electrodes were deposited by vacuum evaporation on the top of the organic active layer through a shadow mask with a channel length of 31 μm and a width of 273 μm. All the devices were annealed at different temperatures (160, 200, 240, 280 ℃) and the transistor performances were tested in air using Keithley 4200 semiconductor parameter analyzer. The mobility was calculated in the saturation regime according to the expression $I_{DS} = (W/2L)\mu_e C_i(V_G - V_{TH})^2$, where I_{DS} is the drain-source current, μ is the field effect mobility, W is the channel width, L is the channel length, C_i is the capacitance per unit area of the gate dielectric layer, and V_{TH} is the threshold voltage.

General procedure for syntheses of PDDP3T-CN and PDPPTPT-CN

A 50 mL flask was charged with 2,5-dibromo-3,4-dicyanothiophene (58.4 mg, 0.2 mmol), monomer **2** (0.2 mmol), $Pd_2(dba)_3$ (9.2 mg, 0.01 mmol), P(o-tolyl)$_3$ (6.1 mg, 0.02 mmol), K_3PO_4 (170.0 mg, 0.8 mmol), catalytic Aliquat 336 and anhydrous toluene (25 mL) under nitrogen atmosphere. The reaction mixture was heated and stirred at 90 ℃ for 48 h. After cooling down to room temperature, the reaction mixture was slowly dropped into 50 mL methanol (containing 1 mL concentrated hydrochloric acid) with vigorous stirring. The precipitate was filtered and extracted by the Sohxlet with methanol, acetone, hexane, dichloromethane, and chloroform successively. The polymer was collected by filtration and dried under vacuum to afford the final product.

PDPP3T-CN: dark-bule solid; Yield, 51%. ^{1}H NMR (400 MHz, $CDCl_2CDCl_2$ (100 ℃), ppm) δ 8.89, 7.73, 4.05, 1.63, 1.39-1.20, 0.80; Anal Calcd for $C_{64}H_{96}N_4O_2S_3$: C 73.27, H 9.22, N 5.34; Found: C 73.00, H 8.91, N 5.08.

PDPPTPT-CN: dark-purple solid; Yield, 76%. ^{1}H NMR (400 MHz, $CDCl_2CDCl_2$ (100 ℃), ppm) δ 8.82, 8.05, 7.81-7.76, 3.98, 1.76, 1.40-1.15, 0.78; Anal Calcd for $C_{64}H_{94}N_4O_2S_2$: C 75.69, H 9.33, N 5.52; Found: C 75.20, H 9.00, N 5.52.

Table 1 Physicochemical properties of polymers **PDPP3T-CN** and **PDPPTPT-CN**

	T_d /°C	λ_{max}(nm)		λ_{edge}(nm)		Mn /kDa	PDI	HOMO /eV	LUMO /eV	E_g^{opt} /eV
		sol	film	sol	film					
PDPP3T-CN	362	824	758	930	950	23.3	2.52	-5.48	-3.80	1.30
PDPPTPT-CN	364	711	705	796	800	67.5	1.80	-5.63	-3.71	1.55

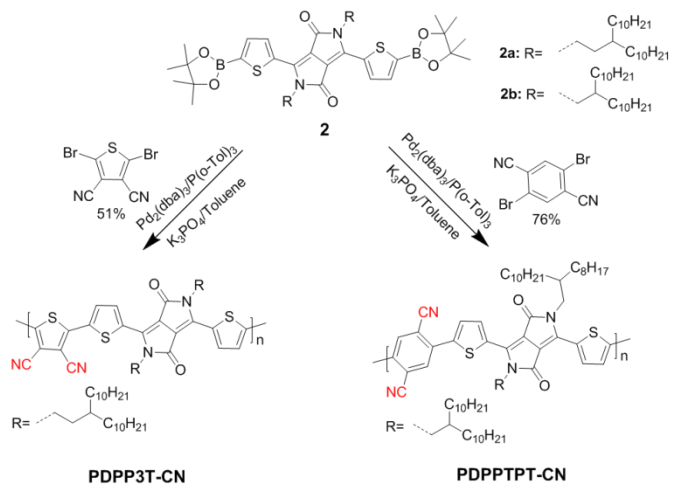

Scheme 2. The synthetic routes for **PDPP3T-CN** and **PDPPTPT-CN**,

Results and Discussion

The synthetic route of copolymers **PDPP3T-CN** and **PDPPTPT-CN** is outlined in Scheme 2. The monomers were synthesized according to the procedures reported in literatures. [27-28] The target polymers **PDPP3T-CN** and **PDPPTPT-CN** were prepared via the Suzuki cross-coupling polymerization. The Suzuki cross-coupling polymerizations were carried out in the presence of the palladium catalyst $Pd_2(dba)_3$, the ligand P(o-tol)$_3$ and the base K_3PO_4 in toluene. The resulting polymers **PDPP3T-CN** and **PDPPTPT-CN** were purified by precipitating in ethanol, followed by Soxhlet extraction with methanol, acetone, hexane and chloroform successively to remove the catalytic impurities and low-molecular-weight moieties. **PDPP3T-CN** was collected as dark-blue solid in a yield of 51%, while **PDPPTPT-CN** was obtained as dark-purple solid in a yield of 76%. Both **PDPP3T-CN** and **PDPPTPT-CN** were soluble in hot chloroform and other chlorinated solvents. The number molecular weight (Mn) of **PDPP3T-CN** and **PDPPTPT-CN** were 23.3 kD and 67.5 kD with polydispersity (PDI) of 2.52 and 1.80 respectively, which were determined by high temperature gel permeation chromatography (GPC) with 1,2,4-trichlorobenzene as the eluent (polystyrene as the standard).

The thermodynamic properties of **PDPP3T-CN** and **PDPPTPT-CN** were studied by thermogravimetric analysis (TGA) and differential scanning calorimetry (DSC). Both **PDPP3T-CN** and **PDPPTPT-CN** exhibited excellent thermal stability with the 5% weight loss up to 360 ℃ under nitrogen atmosphere. DSC curves showed no thermal transition peak was observed for **PDPP3T-CN,** while **PDPPTPT-CN** exhibited discrete endothermic peak at 275 ℃ and exothermic peak at 245 ℃ upon heating and cooling process which might be attributed to the melt of the alkyl chains of polymer.

The frontier orbital energy levels (HOMO and LUMO) of copolymers **PDPP3T-CN** and **PDPPTPT-CN** were evaluated by cyclic voltammetry (CV) technique. As illustrated in figure 1, both **PDPP3T-CN** and **PDPPTPT-CN** showed irreversible oxidation and reduction peaks, respectively. The HOMO and LUMO energy levels calculated from the onset oxidation or reduction potentials with ferrocene as a reference were -5.48/-3.80 eV for **PDPP3T-CN** and -5.63/-3.71 eV for **PDPPTPT-CN**. The HOMO/LUMO energy levels of **PDPP3T-CN** and **PDPPTPT-CN** were lower than the corresponding non-nitrile substituted PDDP3T (HOMO/LUMO: -5.17/-3.61 eV) and PDPPTPT (HOMO/LUMO: -5.35/-3.53 eV), [29-31] indicating the introduction of nitrile group efficiently lowered both HOMO and LUMO levels and was favourable for electron injection to the polymers with respective to the commonly used Au electrode.

The optical properties of **PDPP3T-CN** and **PDPPTPT-CN** were characterized by UV-vis absorption spectroscopy in solutions (hot chlorobenzene) and on thin films (Figure 1). **PDPP3T-CN** exhibited broad absorption band extended from 500 to 950 nm in solution due to the strong intramolecular donor-acceptor charge transfer interactions. Compared to the absorption spectrum in solution, a red-shift of onset absorption (λ_{edge}) and the enhancement of shoulder peak at 745 nm were observed, indicating the strong intermolecular interactions in the films. In contrast, **PDPPTPT-CN** thin film exhibited nearly the same absorption as that of solution, which suggested that molecular aggregation had occurred in solution. The optical band gaps of **PDPP3T-CN** and **PDPPTPT-CN** estimated from λ_{edge} of the thin films were 1.30 and 1.55 eV, respectively.

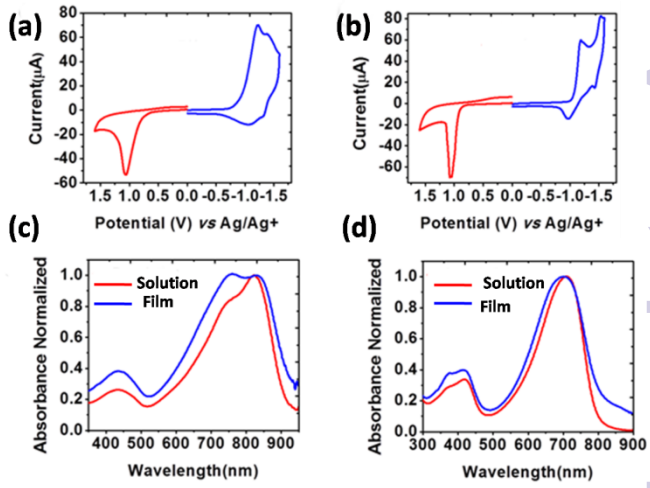

Figure 1. (a-b)Cyclic voltammograms of **PDPP3T-CN** film (a) and **PDPPTPT-CN** film (b) on platinum electrode in CH_3CN solution; (c-d) UV-vis absorption spectra of **PDPP3T-CN** (c) and **PDPPTPT-CN** (b) in solutions and on thin films.

With the aim to evaluate the effect of nitrile group on the charge-carrier transport behaviour of polymers, the electrical properties of **PDPP3T-CN** and **PDPPTPT-CN** were investigated by organic thin film transistors. Bottom-gate/top-contact OTFTs were fabricated on the octadecyltrichlorosilane (OTS)-modified Si/SiO_2 substrates. **PDPP3T-CN** and **PDPPTPT-CN** thin films were spin-coated from $CHCl_3$ solutions (6 mg/mL). The gold source and drain electrodes were evaporated onto the organic semiconductor layer through a shadow mask in high vacuum with a channel length of 31μm

and width of 273μm. The devices were characterized in ambient and the field-effect mobilities calculated from the saturated regime were collected in Table 2.

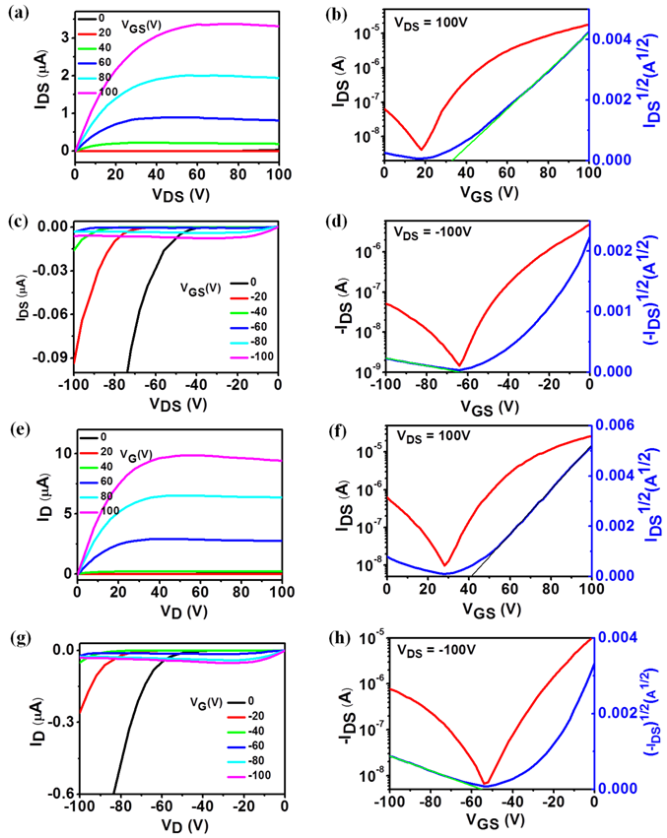

Figure 2 The typical output and transfer curves of **PDPP3T-CN** and **PDPPTPT-CN** based transistors. (a-d) **PDPP3T-CN** based transistors; (e-h) **PDPPTPT-CN** based transistors

Figure 2 showed the typical output and transfer curves of **PDPP3T-CN** and **PDPPTPT-CN** based transistors. **PDPP3T-CN** displayed clear electron-dominant ambipolar charge-carrier transportation characteristics, and the electron mobility was at least one order of magnitude higher than the hole mobility. The as-cast thin films of **PDPP3T-CN** showed an electron mobility of 4.9×10^{-3} $cm^2V^{-1}s^{-1}$ and a hole mobility of 3.9×10^{-4} $cm^2V^{-1}s^{-1}$. With the increase of thermal annealing temperature, the electron mobility of **PDPP3T-CN** improved remarkably, and the highest electron mobility was 0.09 $cm^2V^{-1}s^{-1}$ observed after thermal annealing at 280 ℃. The hole mobility of **PDPP3T-CN** was only increased four times after thermal annealing. It is obvious that the thermal annealing is more helpful to enhance electron mobility. The as-cast thin films of **PDPPTPT-CN** exhibited hole-dominant ambipolar charge-carrier transportation. Interestingly, after thermal annealing **PDPPTPT-CN** based transistors displayed electron-dominant ambipolar charge-carrier transport property. And the highest electron mobility could reach 0.18 $cm^2V^{-1}s^{-1}$ after thermal annealing at 240 ℃. Comparing with the non-nitrile substituted polymers PDPP3T (μ_h= 1.57 $cm^2V^{-1}s^{-1}$, μ_e = 0.18 $cm^2V^{-1}s^{-1}$) and PDPPTPT (μ_h= 0.04 $cm^2V^{-1}s^{-1}$, μ_e = 0.02 $cm^2V^{-1}s^{-1}$) which displayed hole-dominant ambipolar behaviors in inert atmosphere or under vacuum, a remarkable inversion from hole dominated to electron dominated charge-carrier transportation is observed for **PDPP3T-CN** and **PDPPTPT-CN** even in ambient condition. This inversion was mainly attributed to the introduction of nitrile group which lowered the LUMO levels of polymers and facilitated for electron injection from the Au electrode. Hence, the introduction of nitrile groups onto aromatic or heterocyclic core of polymer backbone is an efficient way to obtain high performance n-channel semiconducting polymers.

Table 2.OTFTs characteristics of polymers **PDPP3T-CN** and **PDPPTPT-CN**

Polymers	T_{anneal}(°C)	$\mu_{max}(\mu_{aver})$ ($cm^2v^{-1}s^{-1}$)	V_{th}(V)	$I_{on/off}$
PDPP3T-CN	RT	$4.9\times10^{-3}(3.5\times10^{-3})$(e)	30	3.7×10^{3}
		$3.9\times10^{-4}(3.4\times10^{-4})$(h)	-40	3.2×10^{2}
	160	0.014 (0.01)(e)	33	2.4×10^{3}
		$4.7\times10^{-4}(3.8\times10^{-4})$(h)	-62	3.1×10^{3}
	200	0.032 (0.029)(e)	33	1.3×10^{3}
		$8.9\times10^{-4}(7.2\times10^{-4})$(h)	-64	9.0×10^{1}
	240	0.046 (0.039)(e)	31	2.5×10^{3}
		$1.0\times10^{-3}(8.5\times10^{-4})$(h)	-72	2.6×10^{2}
	280	0.09 (0.076)(e)	34	4.4×10^{3}
		$1.7\times10^{-3}(1.5\times10^{-3})$(h)	-91	2.5×10^{2}
PDPPTPT-CN	RT	$9.2\times10^{-4}(5.7\times10^{-4})$(e)	51	1.2×10^{2}
		$1.5\times10^{-3}(1.0\times10^{-3})$(h)	-50	5.0×10^{2}
	160	0.012 (9.0×10^{-3})(e)	48	9.5×10^{2}
		$3.2\times10^{-3}(2.2\times10^{-3})$(h)	-48	2.0×10^{3}
	200	0.079 (0.062)(e)	52	1.7×10^{3}
		$4.9\times10^{-3}(4.1\times10^{-3})$(h)	-50	2.2×10^{2}
	240	0.18(0.1)(e)	45	4.3×10^{3}
		$8.6\times10^{-3}(7.6\times10^{-3})$(h)	-55	1.1×10^{2}
	280	0.026 (0.022)(e)	44	2.4×10^{3}
		$4.1\times10^{-3}(3.8\times10^{-3})$(h)	-49	1.2×10^{3}

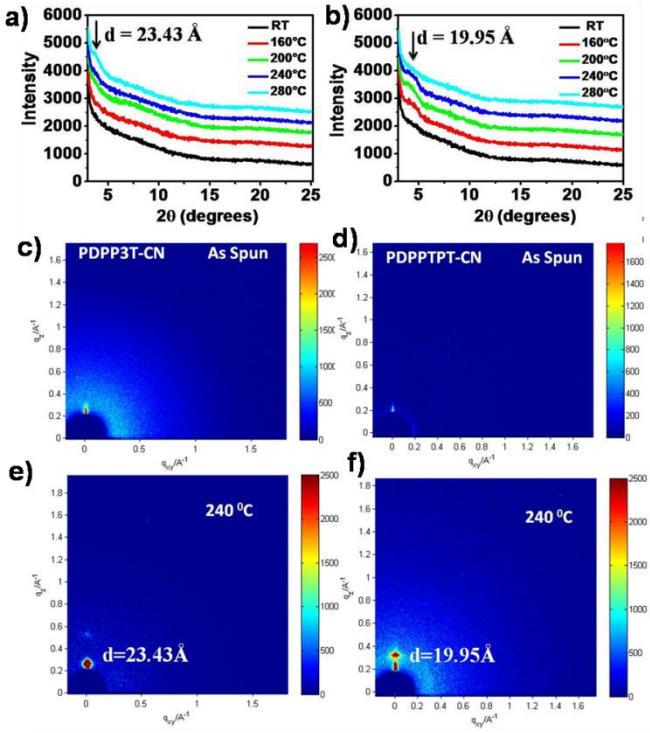

Figure 3 1D-GIXD and2D-XRD patterns of **PDPP3T-CN** and **PDPPTPT-CN** thin films: as-spun and annealed thin films. a), c), e): **PDPP3T-CN**; b), d), f): **PDPPTPT-CN**

The morphology and microstructures of **PDPP3T-CN** and **PDPPTPT-CN** thin films were characterized by atomic-force-microscopy (AFM), 1D X-ray diffraction (1D-XRD) and 2D grazing-incidence X-ray diffraction (2D-GIXD) to shed light on the variation trend of charge-transport characteristics under different annealing temperatures. The AFM images of **PDPP3T-CN** and **PDPPTPT-CN** thin films annealed at different temperatures were shown in supporting information. It can be seen that all the films showed smooth surface with the height scale at 25 nm before and after annealing. The as-spun films of **PDPP3T-CN** displayed well continuity, whereas, small grains were clearly visible after annealed at 160 ℃. Further increasing the annealing temperature to 200 ℃ and 280 ℃, the grains began to coalesce, giving rise to larger grain size and the lamellar morphology with well continuity. 1D-XRD results showed (Figure 3) the films of as-spun and thermal annealed under 240 ℃ were amorphous, while the films annealed at 280 ℃ were crystalline which was proved by the appearance of the diffraction peak. It is well known that the crystallinity is favourable for high charge-carrier transportation, and this is consistent well with the dependence of charge-carrier mobilities of **PDPP3T-CN** on thermal annealing temperatures. For **PDPPTPT-CN**, the trend of the film morphologies on thermal annealing was almost the same as that of **PDPP3T-CN**. The lamellar morphology was gradually formed and the coalescing of grains appeared after thermal annealing (see supporting information). 1D-XRD result revealed the as-spun films of **PDPPTPT-CN** were amorphous. Contrastly to **PDPP3T-CN**, the films of **PDPPTPT-CN** annealed at 160 ℃, 200 ℃, and 240 ℃ were crystalline. However, the diffraction peak sharply disappeared when the film was annealed at 280 ℃. Combined with the improved film morphologies and X-ray diffraction, it is expected that the charge-carrier mobilities of **PDPPTPT-CN** will increase with the increasing of annealing temperature under 240 ℃ and then decrease at higher annealing temperature of 280 ℃, and they actually were. The charge-carrier mobility variation of both **PDPP3T-CN** and **PDPPTPT-CN** thin films is agreeing well with the trend of film morphologies and 1D-XRD results.

2D-GIXD was usually used to probe the molecular packing behaviours in the thin films. Diffraction peaks were observed in the out-of-plane direction (q_z) both for **PDPP3T-CN** (annealed at 280 ℃) and **PDPPTPT-CN** (annealed at 240 ℃). They were indexed as (100) with the d-spacing of 23.43 Å and 19.95 Å for **PDPP3T-CN** and **PDPPTPT-CN**, respectively. This indicated the polymers adopted an edge-on packing motif and formed the layer-by-layer lamellar structures with the polymer backbones standing on the substrate. More important, the d-spacings calculated from XRD were much shorter than the length of polymer with alkyl chains fully extended, suggesting the side alkyl chains were interdigitated between the adjacent layers. [31-32] The remarkable shorter d-spacing of **PDPPTPT-CN** than that of **PDPP3T-CN** suggested the greater degree of alkyl chain interdigitations among **PDPPTPT-CN** molecules.

Conclusions

In summary, polymer semiconductors **PDPPTPT-CN** and **PDPP3T-CN**, containing nitrile-substituted thiophene and benzene building blocks, were synthesized and characterized. Both polymer exhibited ambipolar characteristics in ambient conditions. **PDPP3T-CN** displayed electron dominated ambipolar behaviour with the electron mobility of 0.09 cm^2/Vs and the hole mobility of 0.001cm^2/Vs. The as-spun thin films of **PDPPTPT-CN** showed hole-dominated ambipolar performance and a conversion to electron-dominated ambipolar behaviour was observed after thermal annealing. The highest electron and hole mobilities were 0.18 cm^2/Vs and 0.0086cm^2/Vs respectively, one of the highest electron mobility among DPP-based polymers characterized in ambient condition with bottom-gate/top-contact device configuration. Comparing with the corresponding non-nitrile substituted polymer semiconductors, the introduction of nitrile-substituted aromatic units (i) lowered the LUMO/HOMO energy level of polymers, (ii) led to a remarkable inversion of charge-carrier transportations from hole dominated one to electron dominated one, (iii) strongly improved the ambient stability of the transistors. All these results demonstrated the potential applications of nitrile-substituted aromatic units in high performance polymer semiconductors.

Acknowledgements

This work was supported by National Natural Sciences Foundation of China (21190031, 51273212, 51303201, 21474128) and the "Strategic Priority Research Program" of

the Chinese Academy of Sciences (XDB12010100). H. Li thanks the Shanghai Synchrotron Radiation Facility (beamline BL14B1) for providing the beam time.

Notes and references

1 J. Mei, Y. Diao, L. A. Anthony, L. Fang, Z. Bao, *J. Am. Chem. Soc.* 2013, **135**, 6724.
2 C. Wang, H. Dong, W. Hu, Y. Liu, D. Zhu, *Chem.Rev.* 2012, **112**, 2208.
3 H. Klauk, *Chem. Soc. Rev*. 2010, **39**, 2643.
4 X. Zhao, X. Zhan, *Chem. Soc. Rev*. 2011, **40**, 3278.
5 J. E. Anthony, A. Facchetti, M. Heeney, S. R. Marder, X. Zhan, *Adv. Mater*. 2010, **22**, 3876
6 H. N. Tsao, D. M. Cho, I. Park, M. R. Hansen, A. Mavrinskiy, Y. Yoon do, R. Graf, W. Pisula, H. W. Spiess, K. Müllen, *J. Am. Chem. Soc*. 2011, **133**, 2605
7 X. Zhang, H. Bronstein, A. J. Kronemeijer, J. Smith, Y. Kim, R. J. Kline, L. J. Richter, T. D. Anthopoulos, H. Sirringhaus, K. Song, M. Heeney, W. Zhang, I. McCulloch, D. M. DeLongchamp, *Nat. Commun*. 2013, **4**, 2238.
8 J. Li, Y. Zhao, H. S. Tan, Y. Guo, C. A. Di, G. Yu, Y. Liu, M. Lin, S. H. Lim, Y. Zhou, H. Su, B. S. Ong, *Sci. Rep.* 2012, **2**, 754
9 I. Kang, H. J. Yun, D. S. Chung, S. –K. Kwon, Y. –H. Kim, *J. Am. Chem. Soc*. 2013, **135**, 14896
10 H. Yan, Z. H. Chen, Y. Zheng, C. Newman, J. R. Quinn, F. Dotz, M. Kastler, A. Facchetti, *Nature* 2009, **457**, 679
11 J. H. Park, E. H. Jung, J. W. Jung, H. Jo, *Adv. Mater*. 2013, **25**, 2583
12 T. Lei, J.-H. Dou, X.-Y. Cao, J. -Y. Wang, J. Pei, *J. Am. Chem. Soc.* 2013, **135**, 12168
13 J. Lee, A. R. Han, H. Yu, T. Shin, C. Yang, J. H. Oh, *J. Am. Chem. Soc.* 2013. **135**, 9540
14 T. Lei, J. Dou, Z. Ma, C. Yao, C. Liu, J. Wang, J. Pei, *J. Am. Chem. Soc.* 2012, **134**, 20025
15 G. Kim, S. J. Kang, G. K. Dutta, Y. K. Han, T. J. Shin, Y. Y. Noh, C. Yang, *J. Am. Chem. Soc.* 2014, **136**, 9477
16 T. Lei, X. Xia, J.-Y. Wang, C.-J. Li, J. Pei, *J. Am. Chem. Soc.* 2014, **136**, 2135
17 C. Kanimozhi, N. Yaacobi-Gross, K. W. Chou, A. Amassian, T. D. Anthopoulos, S. Patil, *J. Am. Chem. Soc*. 2012, **134**, 16532.
18 H. J. Yun, S. J. Kang, Y. Xu, S. O. Kim, Y. H. Kim, Y. Y. Noh, S. K. Kwon, *Adv. Mater*. 2014, **26**, 7300-7307
19 J. Zaumseil, H. Sirringhaus, *Chem. Rev*. 2007, **107**, 1296
20 Y. Zhao, Y. Guo, Y. Liu, *Adv. Mater*. 2013, **25**, 5372
21 Z. Liu, G. Zhang, Z. Cai, X. Chen, H. Luo, Y. Li, J. Wang, D. Zhang, *Adv. Mater*. 2014, **26**, 6965
22 X. Guo, A. Facchetti, T. J. Marks, *Chem. Rev*. 2014, **114**, 8943
23 (a) T. Lei, J. Y. Wang, J. Pei, *Acc. Chem. Res.* 2014, **47**, 1117; (b) X. Zhao, L. Ma, L. Zhang, Y. Wen, J. Chen, Z. Shuai, Y. Liu, X. Zhan, *Marcomolecule*s, 2013, **46**, 2152; (c) W. Zhou, Y. Wen, L. Ma, Y. Liu, X. Zhan, *Marcomolecule*s, 2012, **45**, 4115
24 N. S. Cho, D.-H. Hwang, J.-I. Lee, B.-J. Jung, H.-K. Shim, *Macromolecules* 2002, **35**, 1224
25 N. S. Cho, D.-H. Hwang, B.-J. Jung, E. Lim, J. Lee, H.-K. Shim, *Macromolecules* 2004, **37**, 5265
26 M. Wang, J. Li, G. Zhao, Q. Wu, Y. Huang, W. Hu, X. Gao, H. Li, D. Zhu, *Advanced Materials*, 2013**, 25**, 2229
27 J. Y. Balandier, F. Quist, C. Amato, S. Bouzakraoui, J. Cornilb, S. Sergeyev, Y. Geerts, *Tetrahedron*. 2010, **66**, 9560
28 J. Chen, C. Lin, P. Chou, A. Chaskar, K. Wong, *Tetrahedron*. 2011, **67**, 734
29 J. C. Bijleveld, A. P. Zoombelt, S. G. J. Mathijssen, M. M. Wienk, M. Turbiez, D. M. de Leeuw, R. A. J. Janssen, *J. Am. Chem. Soc*. 2009, **131**, 16616
30 X.-R. Zhang, L. J. Richter, D. M. DeLongchamp, R. J. Kline, M. R. Hammond, I. McCulloch, M. Heeney, R. S. Ashraf, J. N. Smith, T. D. Anthopoulos, B. Schroeder, Y. H. Geerts, D. A. Fischer, M. F. Toney, *J. Am. Chem. Soc.* 2011, **133**, 15073
31 J. S. Lee, S. K. Son, S. Song, H. Kim, D. R. Lee, K. Kim, M. J. Ko, D. H. Choi, B. Kim, J. H. Cho, *Chem. Mater*. 2012, **24**, 1316
32 Q. Wu, M. Wang, X. Qiao, Y. Xiong, Y. Huang, X. Gao, H. Li, *Macromolecules*, 2013, **46**, 3887

Nitrile - Substituted Thienyl and Phenyl Units as Building Blocks for High Performance n-Type Polymer Semiconductors

Yu Xiong, Xiaolan Qiao and Hongxiang Li *

Conjugated polymers containing nitrile-substituted thienyl and phenyl units displayed high electron mobility in ambient conditions.